Static and Kinetic Study of a Pressure Induced Order−Disorder Transition: Birefringence and Neutron Scattering

Kalman B. Migler* and Charles C. Han

Building 224, Room B210, Polymers Division, National Institute of Standards and Technology, Gaithersburg, Maryland 20899

Received August 28, 1997; Revised Manuscript Received November 25, 1997

ABSTRACT: We utilize birefringence and neutron scattering to study the statics and kinetics of a pressure-induced order−disorder transition (ODT) in a solvated diblock copolymer. We find that birefringence is an excellent technique to measure the order−disorder transition at high pressure, yielding sharp changes in its intensity at the transition. Small-angle neutron scattering exhibits a corresponding change in the width of the scattering peak at the ODT. Both techniques indicate a nearly linear increase of the ODT temperature as a function of pressure. The combination of pressure as a controlling thermodynamic variable and birefringence as the measurement tool permits short time scale kinetics experiments. We find the time scale of the disordering process to be significantly shorter than the ordering time, as revealed by profound asymmetries in the response of the system upon pressurization compared with depressurization. Disordering times as small as 0.5 s are observed in rapid pressure drop experiments.

Introduction

Diblock copolymers represent a model system for the study of several technologically important areas such as compatibilization, self-assembly and micro-phase transitions. The thermodynamic phase behavior of these systems is quite rich and a variety of ordered structures have been observed.[1−6] The most well studied thermodynamic phase transition is the order−disorder transition (ODT) in which the polymeric molecules self-assemble into a microstructured state. In the case of equal amounts of the A and B polymer (volume fraction $f = 0.5$), the ordered structure is the lamellar state characterized by a one-dimensional periodic modulation of the concentration of the components. The theoretical understanding of this transition is based on Leibler's theory, where the free energy is expanded in terms of a Landau expansion and the random phase approximation is used to generate the structure factor.[7] The parameters of this theory are the volume fraction, f of one of the blocks and χN, where χ is the interaction parameter and N is the number of statistical segments. Fredrickson and Helfand later included fluctuation effects into the theory and found that the disordered region is expanded and the transition is driven to first order.[8]

Experimental work has focused mainly on the variation of f and N through chemical synthesis as well as χ through its temperature dependence.[1−6] Only recently however, have studies examined the effect of pressure on the order−disorder transition in diblock copolymers.[9−14] These studies are part of a larger resurgence of interest in pressure effects in polymer blends, fueled by the advent of in-line small angle scattering techniques, which enable the measurement of pressure dependent microscopic parameters.[15−20] Additionally, pressure-based experiments are technologically important because polymer processing and injection molding are carried out under conditions of high pressure, and it is important to understand the state of the material under processing conditions.

Although there are only a few reports on the effect of pressure on diblock copolymers, several intriguing results have been reported. Hajduk et al.[9] conducted small-angle X-ray scattering experiments on a polystyrene−polyisoprene diblock copolymer and found an increase in the ODT at a rate of 0.2 °C/MPa. However, an attempt to predict this rate based on measured structural parameters yielded an underestimation by a factor or two.[10] Hammouda et al.[11] also found an increase in ODT at rate of approximately 0.2 °C/MPa in a concentrated polystyrene−polyisoprene in the nonpreferential solvent dioctyl phthalate (DOP). Additionally, they observed a pressure induced increase in scattering at low q, defined as $q = (4\pi/\lambda)\sin(\theta/2)$ where θ is the scattering angle and λ is the wavelength of the incident radiation. Frielinghaus et al.[12] studied a poly(ethylene propylene)−poly(ethylethylene) (PEP−PEE) diblock copolymer and found a *decrease* in ODT, which they attributed to a decrease in the enthalpic part of χ. In the diblock (poly(ethylene propylene)−poly(dimethyl siloxane) (PEP−PDMS), Schwahn et al.[13] found reentrant behavior in the phase diagram and a peak in the coil compressibility at the ODT. In a work where pressure was applied to a sample in a mechanical hot press and then cooled and examined in SANS, Bartels et al.[14] found that pressure induced an ordered to disordered transition and speculated that kinetic effects may have played a strong role in their observations.

The above experiments all utilized small-angle scattering techniques to locate the order−disorder transition. However, the transition is often spread out or difficult to determine, especially in experiments with low q resolution such as neutron scattering. Polycrystalline behavior further smears out the difference between the ordered and disordered states near the transition.[21] For example, Frielinghaus et al.[12] found a clear signature of the order to disorder transition in a previously shear aligned sample but not in a "powder average" sample.

* To whom correspondence should be addressed.

S0024-9297(97)01295-3
Published on Web 01/27/1998

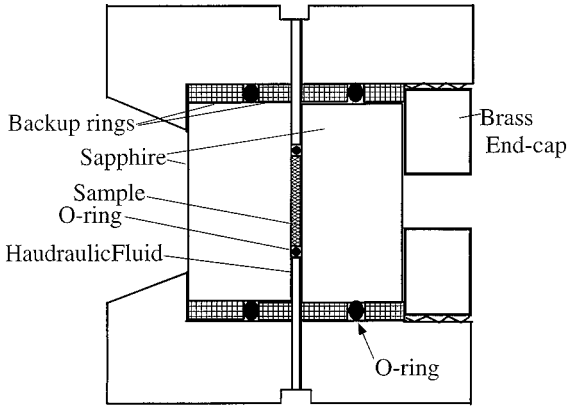

Figure 1. Schematic view of the cross section of the pressure cell that is used in both the optical birefringence and the neutron scattering experiments. The thickness and diameter of the sapphire windows are 38.1 mm and 19 mm, respectively. Pressure is transmitted to the sample via a high-temperature pressure fluid through the sample O-ring. The larger O-rings maintain a seal between the atmosphere and the high-pressure fluid. The cell withstands pressures up to 130 MPa and temperatures up to 200 °C. This drawing is not to scale.

Typically, an independent measurement of the order−disorder transition is used to measure the ODT. At atmospheric pressure, rheological techniques are used because there is a discontinuity in the low-frequency elastic modulus.[22] This technique would be quite difficult to carry out at high pressures. Thus an alternative technique is needed to measure the ODT under high-pressure conditions.

We find that birefringence experiments are an excellent complement to scattering for measurement of the ODT under pressure. In temperature based experiments at atmospheric pressure, distinctive features in optical birefringence have been observed upon passing through the ODT.[23−26] An additional advantage (relative to rheology) is that the sample is not mechanically disturbed by the measurement itself. A rheological measurement of ODT must always contend with the possibility of a shear induced shift in phase behavior, as is frequently observed in complex fluids.[27] Furthermore birefringence is an inherently simple technique.

A significant feature of pressure as a controlling thermodynamic parameter is that very fast changes in the state of the system can be affected. Since birefringence measurements can be made quite rapidly, it is a natural match for a pressure jump experiment. This opens up a new realm of kinetics studies of the ODT.

Experimental Setup

The pressure cell is designed to allow both optical and neutron scattering studies of materials under conditions that are typical of polymer processing. The maximum pressure of 120 MPa is greater than that encountered in most processing operations while the maximum temperature of 200 °C is typical for many materials. The pressure cell was custom manufactured by Temco, Inc.[28] and is shown schematically in Figure 1. Other groups have also built pressure cells for various types of scattering experiments.[9,16,20,29,30] In our experiments, we utilize sapphire windows because of their mechanical strength and transparency to both neutrons and optical radiation. The dimensions of each sapphire window used (38.5 mm diameter by 19 mm thick) are based on a safety calculation which utilizes the maximum pressure and unsupported area. The sample is sandwiched between the two sapphire windows which are maintained at a 1 mm separation by a stainless steel spacer. Laterally, the sample is contained by a viton O-ring, whose undeformed dimensions are 1.5 mm thick by 17 mm diameter. The function of the O-ring is to transmit pressure from the hydraulic fluid to the sample while maintaining a seal between the two fluids. The O-ring is compressed to a 1 mm thickness by the windows when the cell is assembled. The hydraulic fluid is Dow Corning 710 silicone fluid,[28] chosen for its high temperature thermal stability. The diameter of the O-ring (17 mm) is large compared to the cadmium mask limited diameter of the neutron beam (10 mm) in order to prevent the O-ring from entering the beam upon application of pressure.

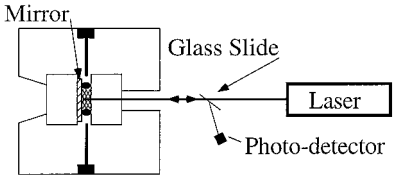

Figure 2. Optical arrangement for use in birefringence measurement. The use of a mirror and glass slide oriented at the Brewster angle circumvents the birefringence problem of the sapphire. The optical signal detection, as well as the pressure and temperature, is computer controlled.

Pressure is applied by a computer-controlled pressure generator from Advanced Pressure Products[28] which incorporates a motor-driven piston in conjunction with feedback from a pressure transducer. The home-built controlling software can work either in a constant pressure mode or in a pressurization rate mode. In these experiments, the pressurization rate is varied between 6.9×10^{-4} and 3.1 MPa/s. For depressurization experiments, the maximum rate is approximately −100 MPa/s, achieved by opening a pressure valve to atmospheric pressure. Temperature control to within 0.1 °C of the setpoint is achieved with a Watlow band heater connected to an Omega temperature controller system.[28] The band heater surrounds the pressure cell and the controlling thermocouple is located in the body of the cell. For automated runs, the temperature controller is interfaced to a computer.

The configuration used for optical birefringence measurements is shown in Figure 2. To prevent the birefringence (and the stress induced birefringence) of the sapphire from influencing the data, we use a reflection based optical scheme. Light from a helium−neon laser is polarized by a crystal polarizer so that the **E** field vector is in the plane of Figure 2. The light then passes through a microscope slide which is oriented at the Brewster angle so that there is no reflected light at this interface. The light hits the front sapphire window which is oriented so that one of its crystal axes is aligned with the direction of the incident **E** field. Under this condition, the polarization of the light passing through the sapphire is not affected. Light passes through the sample, reflects off the mirror, and passes back through the sample and front sapphire window and then to the slide oriented at the Brewster angle. If the sample is isotropic, the polarization of the light is still in the plane of the experiment and no light will be reflected off the Brewster slide into the photodetector. However, if the sample is birefringent, then a portion of the light will be reflected into the photodetector in accordance with Snell's law. An additional sheet polarizer oriented to only allow passage of vertically polarized light was placed in front of the photodetector. We tested the optical system with only an isotropic fluid in the pressure cell (the hydraulic fluid) and found that only residual quantities of light entered the photodetector, and this response was minimally changed by the application of heat and pressure. The power meter of the photodetector is also interfaced to the computer allowing automated data collection.

The sample is a perdeuterated polystyrene−polybutadiene block copolymer; each block has a number averaged relative molecular mass of 10 000. This material was synthesized in the laboratory of J. Mays. To lower the ODT, we solvate the material in dioctyl phthalate at a polymer mass fraction of 68.5%.

The neutron scattering studies were carried out on the 8 m small-angle scattering instrument at the National Institute

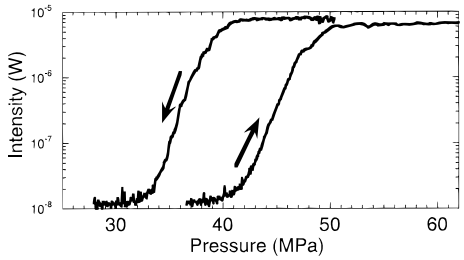

Figure 3. Plot of birefringence vs pressure for the PS−PB diblock in DOP. The temperature is 86 °C and the pressurization rate is 6.9×10^{-4} MPa/s. The sample is in the ordered state when the birefringence is above the baseline. The hysteresis between ordering and disordering is (9 ± 2) MPa.

of Standards and Technology. The wavelengths used were between 9 and 15 Å; the resolution is $\Delta\lambda/\lambda = 0.25$. The collected data were corrected for background noise, sapphire scattering and detector inhomogeneities. The absolute intensity was calculated by comparison to a secondary silica standard.

Birefringence Measurement of ODT

As mentioned previously, there have been several experiments that used birefringence to measure the order−disorder temperature in diblock copolymers. These experiments revealed sharp changes in birefringence as the system orders or disorders. The theory for the birefringence of randomly oriented lamellar diblocks near the ODT has been constructed.[23,24] Balsara et al.[23] consider a collection of randomly oriented birefringent grains and calculate the total birefringence for light propagating through the sample. In the limit of small birefringence they obtain

$$\frac{I}{I_0} = \frac{4\pi^2}{15}(\Delta n)^2 \frac{L l_{av}}{\lambda_{opt}{}^2} \tag{1}$$

I/I_o is the relative transmitted power, Δn is the form birefringence, L is the thickness of the sample, l_{av} is the average grain size, and λ_{opt} is the wavelength of light. Near the ODT, where chain stretching is small, the form birefringence is expected to be larger than the intrinsic birefringence. Amundson et al.[24] found that

$$\Delta n \approx \overline{\langle \Psi \rangle^2} \tag{2}$$

where $\Psi(\mathbf{r})$ is an order parameter defined as the deviation of the composition of one species from its mean value. The brackets represent a time average and the bar represents a spatial average. Equations 1 and 2 indicate that the birefringence varies linearly in the average grain size and is proportional to the *fourth* power of Ψ.

Figure 3 shows the results of an experiment in which the temperature of the sample is constant (86 °C) and pressure is ramped up and down. In this case, the pressure is changed at a rate of 6.9×10^{-4} MPa/s; thus the total time for the two runs of Figure 3 is 16 h. At 86 °C and atmospheric pressure, this sample is in the disordered state; thus the birefringence is zero. As the pressure is increased, there are two characteristic pressures. The first one marks the onset of the birefringence, which occurs in this case at 40 ± 2 MPa.[31] The birefringence increases rapidly with pressure over a narrow range until a knee in the curve occurs at 50 ± 4 MPa, which marks the second characteristic pressure. Above this pressure, the birefringence signal saturates

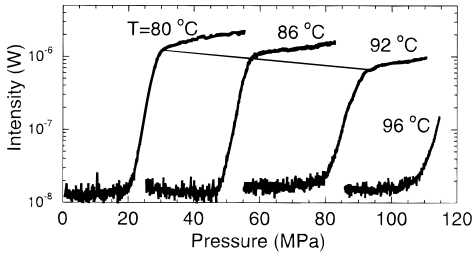

Figure 4. Measurement of the pressure-induced ordering transition for four temperatures via the birefringence technique. The pressurization rate is 6.9×10^{-3} MPa/s. The amplitude of the birefringence is a strong function of the pressure at which the order−disorder transition occurs. The disordering transition proceeds in a similar manner as shown in Figure 3, although the hysteresis is larger due to the larger pressurization rate.

or increases at a slower rate. Upon depressurization, the shape of the curve is quite similar and we find a hysteresis of 9 ± 2 MPa in comparing the onset of ordering and disordering. Recently, Balsara et al. studied the growth of ordered grains (cylindrical microstructure) upon passing through the ODT.[25] They found two regimes: the first in which the birefringence grows rapidly due to the formation and growth of grains and a second in which the grains fill the sample and slowly evolve. We believe that the two regimes seen in our birefringence measurements upon ordering correspond to those studied by Balsara et al.

The first question to address is the location of the order−disorder point for a given birefringence curve. Using the criteria that an isotropic fluid exhibits no birefringence and that only an ordered fluid can exhibit optical anisotropy, the location of the ODT is the point where the birefringence first shows an observable increase (in the case of ordering). One concern is whether pretransitional fluctuations can give rise to an increase in birefringence. Current theoretical models claim that the order of magnitude of the correlation length of a sample which is in the disordered state, but near the ODT, is one radius of gyration. Due to the small length scale of this anisotropy relative to the wavelength of light, we do not expect to observe birefringence in the pre-transition region. Thus we mark the onset of the ODT by the point at which the birefringence signal first deviates from the baseline signal.

The experimental protocol used in these optical experiments is similar to cloud point measurements. The pressure is scanned at a preset rate, but instead of observing changes in scattered intensity, we observe changes in sample birefringence. In any type of scanning experiment, it is critical to know the response rate of the sample compared to the scan rate of the experiment. The relation between kinetics and pressurization is discussed in detail in the kinetics section.

In Figure 4 we extend the measurements described above to a range of temperatures, from 80 to 96 °C. For clarity, four representative curves are shown of the pressure induced ordering transition. The melting of the ordered phase upon depressurization proceeds in a manner similar to that shown in Figure 4; i.e., the shape is similar but there is a hysteresis. In this data set, the pressurization rate is 10 times larger than shown in Figure 3, with a correspondingly larger hysteresis of 14 ± 2 MPa.

The data show several features. First, as the temperature increases, the amount of pressure needed to

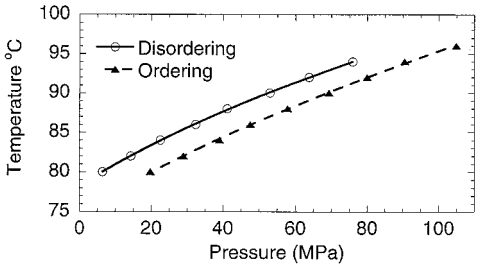

Figure 5. Measurement of the change in the order−disorder transition temperature as a function of pressure. The hysteresis of (14 ± 2) MPa is constant throughout the pressure range. The uncertainty in the data points is ±2 MPa.

induce the ordering clearly increases. Second, the amplitude of the birefringence decreases as the temperature increases, as shown by the straight line drawn through the "knee" of the birefringence curves.

Kinetic effects are an important factor causing the decrease in the amplitude of the birefringence at elevated pressures. As the viscosity of the diblock is an increasing function of pressure and the growth of domains requires considerable molecular reorientation, we speculate that this is the major cause in the reduced amplitude at elevated pressures. The controlling factor in the viscosity is probably the polystyrene block, as T_g is an increasing function of pressure.

Utilizing the full data set represented by Figure 4 and similar data for the depressurization curves, the order−disorder line is drawn in the pressure−temperature plane. In Figure 5 the temperature of the ODT is plotted on the vertical axis to allow comparison to other work. While this plot is nearly linear, there is negative curvature to this line. The initial slope of the line is $dT_{ODT}/dP = 0.25 \pm 0.02$ MPa/°C. At a slower scan rate, we expect that the disordering curve would remain unchanged but the ordering curve would be shifted to lower pressures, reducing the hysteresis. These effects are discussed in the kinetics section.

Neutron Scattering

Neutron scattering is a powerful tool to extract information at length scales on the order of polymer molecular dimensions. One of the major purposes of this experiment is to correlate our neutron scattering measurements with those obtained from birefringence. SANS experiments were conducted separately on the same diblock material as was used in the birefringence experiment. The protocol for the SANS experiments is to work in a stepwise fashion where the temperature is kept constant and the pressure is incremented in set jumps ΔP (typically $\Delta P = 6.9$ or $\Delta P = 10.35$ MPa). At a given temperature, the pressure is incremented. For each pressure, the sample is allowed to equilibrate for 20 min prior to data acquisition. For the run at 86 °C, measurements were acquired for both pressurization and depressurization. At the other temperatures, only the pressurization data were acquired.

Figure 6 shows a typical plot of the increase in $I(q)$ as pressure is applied to the system. At ambient pressure the material is in the disordered phase. As pressure is applied, the peak intensity $I(q^*)$ increases while the width of the peak decreases. Additionally, we observe a small decrease in the peak position, q^* as the system is pressurized, indicating an expansion of the domains. To locate the order−disorder transition, we measure the changes in the width of the peak of $I(q)$.

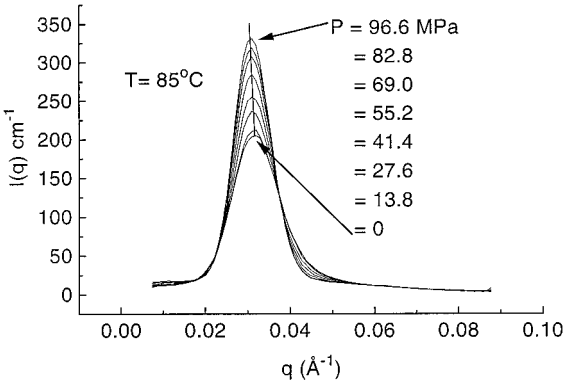

Figure 6. Small-angle neutron scattering study of the pressure induced ordering transition. In this run, the temperature is 85 °C and the pressure is incremented in jumps of 6.9 MPa increments (for clarity, half of the curves are omitted). In the corresponding depressurization experiment, there is a hysteresis of 9 MPa.

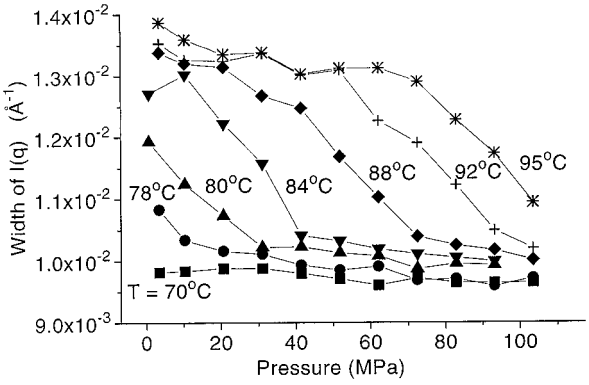

Figure 7. Plot of width of the scattering peaks (full width at half-maximum) as a function of pressure for a series of temperatures from 70 to 95 °C. Half the curves are omitted for clarity. The order−disorder transition occurs somewhere in the region where the width is decreasing most strongly. The uncertainty in the data points is $\pm 2 \times 10^{-4}$ Å^{-1}. In these data series, the pressure is incremented in steps of 10.35 MPa

This approach has been used previously to locate the ODT—it is often a more sensitive indicator than an analysis of $I(q^*)$.[32−34] The results of a series of measurements at different temperatures and pressures is shown in Figure 7. From this plot, it is clear that as the pressure increases and the ordering point is approached, the width of the peak decreases and then levels off at a value of approximately 1.0×10^{-2} Å^{-1}. A hysteresis of 9 ± 2 MPa was observed for the data run of 86 °C when cycling the pressure from 0 to 100 MPa and back. This is the same value that was found in the birefringence experiment carried out at the slowest scan rate.

To directly compare the SANS results with those from birefringence, we superimpose in Figure 8 the birefringence and SANS data for an experiment carried out under the same conditions of pressure and temperature but albeit different protocols. We present results for a depressurization experiment because these are much less sensitive to pressure scan rate (see *Kinetics* section). The vertical dashed line in Figure 8 indicates the disordering transition point as revealed by birefringence. The disordering point occurs somewhere in the midrange of the region in which the SANS peak width exhibits a large change in size. The comparison of these two curves indicates that, for the SANS data, it is reasonable to assign the ODT to the midrange of the

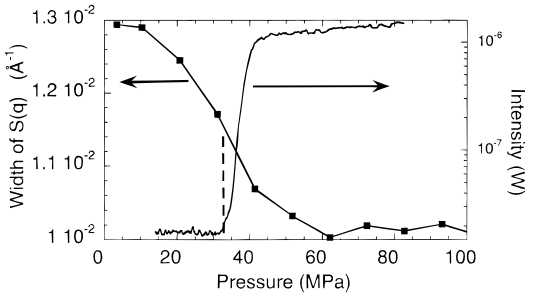

Figure 8. Birefringence intensity and SANS peak width as a function of pressure during a depressurization experiment at $T = 86$ °C. This allows a direct comparison of the two techniques for sensitivity to the ODT.

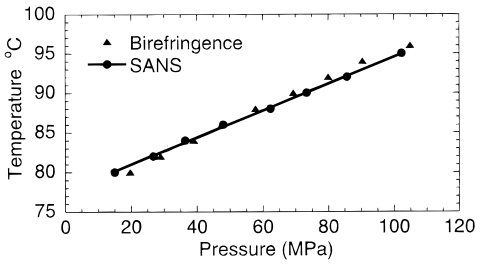

Figure 9. Comparison of the temperature−pressure ODT line as measured by birefringence and SANS.

drop in peak width. Other measures such as the maximum negative slope could also be used. Using the midrange criterion, the pressure induced ODT as measured by SANS is compared to that measured by birefringence in Figure 9. While the agreement is good, there are some differences. The SANS data are best fit by a linear increase in the ODT temperature as a function of pressure at a rate of $dT_{ODT}/dP = 0.17 \pm 0.02$ MPa/°C, whereas the birefringence fit included as small quadratic correction. We cannot account for this small discrepancy.

Kinetics

The study of the kinetics of the order−disorder transition is greatly facilitated by the use of pressure as the thermodynamic control variable because of the wide range of pressurization rates. Furthermore, the use of a birefringence measurement technique allows for rapid data acquisition. The combination of these two methods should allow the study of fast processes. Previous kinetics work has examined both ordering and disordering transitions by the temperature jump method.[35−37] Typically, from 15 to 100 s is used to achieve thermal equilibrium.

In Figure 10 we demonstrate the importance of the scan rate in the ordering process by changing the pressurization rate by several orders of magnitude, from 6.9×10^{-4} 1 MPa/s to 3.1 MPa/s. The first feature to note is that the onset of birefringence is strongly dependent on the pressurization rate. At the lowest pressurization rate, the onset of birefringence occurs at 40 ± 2 MPa, while at the highest pressurization rate (3.1 MPa/s), the onset of birefringence has not occurred by the time that the pressure has reached 110 MPa. The next feature to note is that the amplitude of the birefringence increases strongly as the scan rate decreases. The slowest scan rate of 6.9×10^{-4} MPa/s represents the curve which is closest to equilibrium.

While the observation of the ordering transition is highly dependent on the pressurization rate, the observation of the disordering transition is remarkably rate independent. In Figure 11, we show the depressurization curves corresponding to the slowest and fastest rates of Figure 10. We find that the disordering transition occurs at the same pressure.

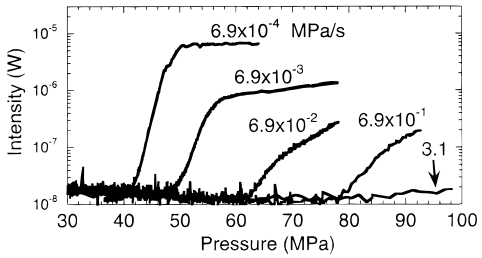

Figure 10. Demonstration of the effect of the pressurization rate on the observation of the ordering transition during pressurization. In contrast the corresponding depressurization experiment shows very little variation of the disordering transition with the rate.

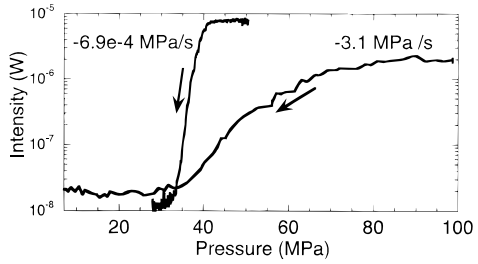

Figure 11. Demonstration of the insensitivity of depressurization rate to the disordering transition. While the depressurization rate ratio of the two curves is greater than 4000, the point at which the birefringence drops to its baseline level is the same.

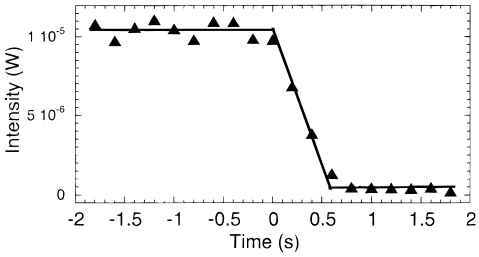

Figure 12. Kinetics of the disordering process in an uncontrolled pressure release experiment. At $t < 0$ s, the pressure and temperature are 54.5 MPa and 86 °C, respectively. At $t = 0$ s, a pressure valve is opened to the atmosphere, causing the pressure to drop to zero within 0.5 s.

As an extreme example of speed at which disordering can occur, we show in Figure 12 the fastest depressurization experiment at a rate of approximately −100 MPa/s, achieved by opening a pressure valve to atmospheric pressure. In this plot, at time $t < 0$ s, the temperature is 86 °C and the pressure is 54.5 MPa; thus conditions are well within the ordered phase. At $t = 0$ s, a pressure valve is released, bringing the sample conditions into those of the disordered state. The birefringence shows clearly that the sample disorders in 0.5 ± 0.1 s, at a rate even faster than that of the measured depressurization. By the time the pressure reaches 10 MPa, the birefringence signal has already reached its baseline value.

Figure 11 shows that the fastest and slowest pressurization rates yield the same disordering points. Returning to Figure 5, it is now clear that the disordering curve is unaffected by pressurization rate whereas

the ordering curve would be shifted to lower pressures if the pressurization rate were lower. Consequently the hysteresis is highly pressurization rate dependent; at the slowest pressurization rate, it is 9 ± 2 MPa (as seen in Figure 3), increasing to 14 ± 2 MPa at a pressurization 10 times greater.

At high-pressure pressurization rates, we need to consider the effects of adiabatic heating or cooling. The expression for the differential temperature change induced by a differential pressure change is[38]

$$dT = \frac{T v \alpha}{C_p} dP \tag{3}$$

where v is the specific volume and C_p is the isobaric specific heat. Using values typical of polymeric materials, we obtain a jump of approximately -4 °C for the sudden jump from 54.5 to 0 MPa. In terms of the ODT, this negative temperature jump tends to induce *order* whereas the depressurization tends to induce *disorder*. Clearly, the pressure effect is stronger in this case. In the pressurization experiments discussed in Figure 10, adiabatic effects must be discussed in relation to the conductive heating time

$$t_c = \frac{d^2}{\alpha} \tag{4}$$

where d is the thickness, and α is the thermal diffusivity. Using $d = 1$ mm and a typical value of $\alpha = 5 \times 10^{-7}$ m^2/s, we get $t_c \approx 2$ s. These relations indicate that adiabatic heating and cooling is negligible for all but the for the fastest pressurization rate.

The profound asymmetry between the ordering and disordering time scales is a natural consequence of the different dynamics between these two processes. In a first order ordering process, nucleation of a grain of a critical size must first occur, followed by its growth. This is a collective process. In contrast, for disordering, once the system is unstable, the time scale is governed by a Rouse time for an individual molecule, which need only to rearrange itself.

Conclusion

In this work, we utilize birefringence and neutron scattering to study the effect of pressure on the order−disorder transition in a solvated block copolymer system. We find that birefringence is noninvasive high-precision technique which allows for measurement of both static and fast kinetic processes. Both techniques indicate a nearly linear increase of the ODT temperature as a function of pressure. Birefringence, due to its greater sensitivity, can measure deviations from linearity at higher pressures. The width of the SANS scattering peak does show a clear decrease upon ordering, but it is spread out by about 40 MPa. These measurements yield a similar sign and magnitude to those carried out on polystyrene−polyisoprene. In the kinetics experiments which utilize birefringence, disordering times as fast as 0.5 s are observed in rapid pressure drop experiments. In contrast, the growth of the ordered phase is slower to due its collective nature.

Acknowledgment. We wish to acknowledge J. Mays for synthesizing the samples used in this experiment.

References and Notes

(1) Wolf, T.; Burger, C.; Ruland, W. *Macromolecules* **1991**, *24*, 958.
(2) Schulz, M. F.; Bates, F. S.; Almdal, K.; Mortensen, K. *Phys. Rev. Lett.* **1994**, *73*, 86.
(3) Bates, F. S.; Schulz, M. F.; Khandpur, A. K.; Förster, S.; Rosedale, J. H.; Almdal, K.; Mortensen, K. *Faraday Discuss.* **1994**, *98*, 7.
(4) Hashimoto, T.; Ijichi, Y.; Fetters, L. *J. Chem Phys.* **1998**, *89*, 2463.
(5) Hamley, I. W.; Koppi, K. A.; Rosedale, J. H.; Bates, F. S.: Almdal, K.; Mortensen, K. *Macromolecules* **1993**, *26*, 5959.
(6) Koberstein, J. T.; Russell, T. P.; Walsh, D. J.; Pottick, L. *Macromolecules* **1990**, *23*, 877.
(7) Leibler, L. *Macromolecules* **1980**, *13*, 1602.
(8) Fredrickson, G.; Helfand, E. *J. Chem. Phys.* **1987**, *87*, 697.
(9) Hajduk, D. A.; Gruner, S. M.; Erramilli, S.; Register, R. A.; Fetters, L. J. *Macromolecules* **1996,** *29*, 1473.
(10) Hajduk, D. A.; Urayama, P.; Gruner, S. M.; Erramilli, S.; Register, R. A.; Brister K.; Fetters L. J. *Macromolecules* **1995,** *28*, 7148.
(11) Hammouda, B.; Lin, C. C.; Balsara, N. P. *Macromolecules* **1995**, *28*, 4765.
(12) Frielinghaus, H.; Schwahn, D.; Mortensen, K.; Almdal, K.; Springer, T. *Macromolecules* **1996,** *29*, 3263.
(13) Schwahn, D.; Frielinghaus, H.; Mortensen, K.; Almdal, K. *Phys. Rev. Lett.* **1996,** *77*, 3153.
(14) Bartels, V. T.; Stamm, M. ; Mortensen, K. *Polym. Bull.* **1996**, *36*, 103.
(15) Janssen, S.; Schwahn, D.; Mortensen, K.; Springer, T. *J. Phys. IV* **1993,** *C8*, 3.
(16) Janssen, S.; Schwahn, D.; Mortensen, K.; Springer, T. *Macromolecules* **1993,** *26*, 5587.
(17) Schwahn, D.; Schmackers, T.; Mortensen, K. *Phys. Rev. E* **1995,** *52*, 1288.
(18) Janssen, S.; Schwahn, D.; Springer, T.; Mortensen, K. *Macromolecules* **1995,** *28*, 2555.
(19) Hammouda, B.; Benmouna, M. *J. Polym. Sci., Polym. Phys.* **1995**, *33*, 2359.
(20) Hammouda, B.; Bauer, B. J. *Macromolecules* **1995,** *28*, 4505.
(21) Balsara, N. P.; Perahia, D.; Safinya, C. R.; Tirell ,M.; Lodge, T. P. *Macromolecules* **1992**, *25*, 3896.
(22) Rosedale, J. H.; Bates, F. S. *Macromolecules* **1990**, *23*, 2329.
(23) Balsara, N. P.; Garetz, B. A.; Dai, H. J. *Macromolecules* **1992**, *25*, 6072.
(24) Amundson, K.; Helfand, E.; Patel, S. S.; Quan, X; Smith, S. D. *Macromolecules* **1992**, *25*, 1935.
(25) Dai, H. J.; Balsara, N. P.; Garetz, B. A.; Newstein, M. C. *Phys. Rev. Lett.* **1996**, 77, 3677.
(26) Floudas, G.; Fytas, G.; Hadjichristidis, N.; Pitsikalis, M. *Macromolecules* **1990**, *28*, 2359.
(27) Larson, R. G. *Rheol Acta* **1992**, *31*, 497.
(28) Certain equipment and instruments or materials are identified in this paper in order to adequately specify the experimental conditions. Such identification does not imply recommendation by the National Institute of Standards and Technology, nor does it imply that the materials are necessarily the best available for the purpose.
(29) Kiran, E.; Zhuang, W. H. *J. Supercrit. Fluids* **1994,** *7*, 1.
(30) Szydlowski, J.; Rebelo, L. P.; Vanhook, W. A. *Rev. Sci. Instrum.* **1992,** *63*, 1717.
(31) Quoted uncertainties in this work represent the best estimate of two standard deviations in the experimental uncertainty.
(32) Winey, K. I.; Gobran, D. A.; Xu, Z.; Fetters, L. J.; Thomas, E. L. *Macromolecules* **1994**, *27*, 2392.
(33) Floudas, G.; Pakula, T.; Fischer, E. W.; Hadjichristidis, N.; Paspas, S. *Acta Polym.* **1994**, *45*, 176.
(34) Hashimoto, T.; Ogawa, T.; Han, C. D. *J. Phys. Soc. Jpn* **1994**, *63*, 2206.
(35) Floudas, G.; Fytas, G.; Hadjichristidis, N.; Pitsikalis, M. *Macromolecules* **1995**, *28*, 2359.
(36) Hashimoto, T.; Sakamoto, N. *Macromolecules* **1995**, *28*, 4779.
(37) Russel, T. P.; Chin, I. *Colloid Polym. Sci.* **1994** *272*, 1373.
(38) Callen, H. *Thermodynamics;* John Wiley and Sons: New York, 1966.

MA971295C